MICROCOPY RESOLUTION TEST CHART

NATIONAL BUREAU OF STANDARDS-1963-A

The Solar Coronal X-Ray Spectrum from 15.4 to 23.0 Angstroms: Lines from Highly Ionized Calcium and Chromium and Their Usefulness as Plasma Diagnostics
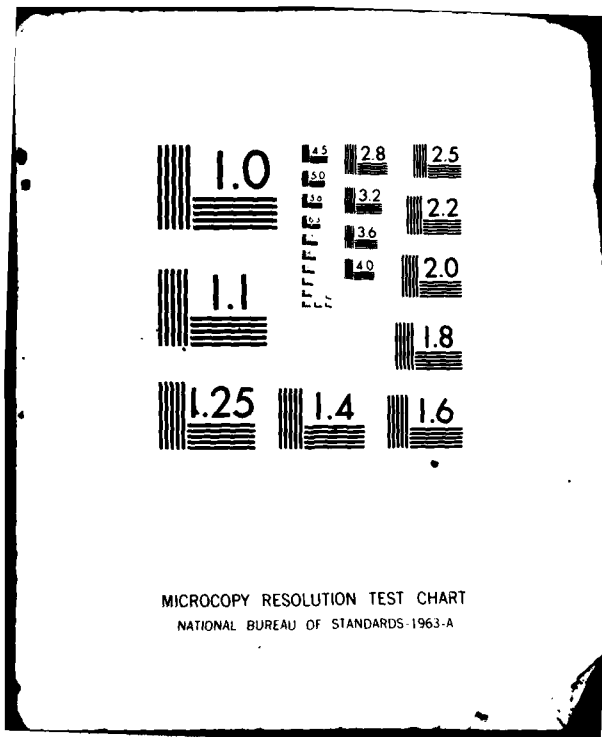
Prepared by

D. L. McKENZIE and P. B. LANDECKER
Space Sciences Laboratory
Laboratory Operations
The Aerospace Corporation
El Segundo, Calif. 90245

7 January 1982

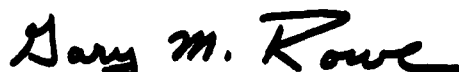DTIC
SELECTED
MAR 8 1982

82 03 08 038

This report was submitted by The Aerospace Corporation, El Segundo, CA 90245, under Contract No. F04701-81-C-0082 with the Space Division, Contracts Management Office, P.O. Box 92960, Worldway Postal Center, Los Angeles, CA 90009. It was reviewed and approved by The Aerospace Corporation by G. A. Paulikas, Director, Space Sciences Laboratory. Captain Gary M. Rowe, SD/YLT , was the project officer for Mission-Oriented Investigation and Experimentation (MOIE) Programs.

This report has been reviewed by the Public Affairs Office (PAS) and is releasable to the National Technical Information Service (NTIS). At NTIS, it will be available to the general public, including foreign nations.

This technical report has been reviewed and is approved for publication. Publication of this report does not constitute Air Force approval of the report's findings or conclusions. It is published only for the exchange and stimulation of ideas.

Gary M. Rowe, Captain, USAF
Project Officer

Flc Ian P. Meinhardt, Lt Col, USAF
Director of Advanced Space Development

FOR THE COMMANDER

Norman W. Lee, Jr., Colonel, USAF
Deputy for Technology

REPORT DOCUMENTATION PAGE		READ INSTRUCTIONS BEFORE COMPLETING FORM
1. REPORT NUMBER SD-TR-82-06	2. GOVT ACCESSION NO. AD-A111 740	3. RECIPIENT'S CATALOG NUMBER
4. TITLE (and Subtitle) THE SOLAR CORONAL X-RAY SPECTRUM FROM 15.4 TO 23.0 ANGSTROMS: LINES FROM HIGHLY IONIZED CALCIUM AND CHROMIUM AND THEIR USEFULNESS AS PLASMA DIAGNOSTICS		5. TYPE OF REPORT & PERIOD COVERED
		6. PERFORMING ORG. REPORT NUMBER TR-0082(2940-01)-2
7. AUTHOR(s) David L. McKenzie and Peter B. Landecker		8. CONTRACT OR GRANT NUMBER(s) F04701-81-C-0082
9. PERFORMING ORGANIZATION NAME AND ADDRESS The Aerospace Corporation El Segundo, Calif. 90245		10. PROGRAM ELEMENT, PROJECT, TASK AREA & WORK UNIT NUMBERS
11. CONTROLLING OFFICE NAME AND ADDRESS Space Division Air Force Systems Command Los Angeles, Calif. 90009		12. REPORT DATE 7 January 1982
		13. NUMBER OF PAGES 35
14. MONITORING AGENCY NAME & ADDRESS(if different from Controlling Office)		15. SECURITY CLASS. (of this report) Unclassified
		15a. DECLASSIFICATION/DOWNGRADING SCHEDULE

16. DISTRIBUTION STATEMENT (of this Report)

Approved for public release; distribution unlimited

17. DISTRIBUTION STATEMENT (of the abstract entered in Block 20, if different from Report)

18. SUPPLEMENTARY NOTES

19. KEY WORDS (Continue on reverse side if necessary and identify by block number)

Spectrum: X-ray; Element Abundances, Plasma Diagnos'
Solar X-ray

20. ABSTRACT (Continue on reverse side if necessary and identify by block number)

Observations by the SOLEX experiment from the USAF P78-1 satellite are used to examine the 15.4 - 23.0 Å X-ray spectrum from both flaring and nonflaring solar active region plasmas. High sensitivity, attained by summing data from several successive spectral scans, enabled the detection of more than 60 lines in this wavelength region. Most of the lines expected to be strongest from Cr XV-XVI and Ca XV-XVIII were detected; those undetected were obscured by blending. In addition, a blend of two Cr XVIII lines was observed, and three

19. KEY WORDS (Continued)

20. ABSTRACT (Continued)

Cr XVII lines are tentatively identified. Lines from higher ionization states of Cr are at shorter wavelengths and are hard to detect because of strong Fe emission. The Cr and Ca spectra are similar to those of isoelectronic species of Fe. The Cr XV $2p^6$ $^1S_0$ − $2p^5 3d$ $^1P_1$ (18.497 Å) line is sufficiently strong that it can be used for analysis of both flaring and nonflaring plasmas. Calculations of the collision strength from the ground state to the $2p^5 3d$ $^1P_1$ level and of the Cr ionization equilibrium are needed for optimum use of this line. Theoretical data for the Ca XVI $2p$ $^2P_{1/2}$ − $3d$ $^2D_{3/2}$ line are available, but the line is too weak to be useful for analysis of nonflaring plasmas. Furthermore, the line is density-sensitive for electron density $n_e > 10^{11}$ cm^{-3} but is not a good density diagnostic because no non-density-sensitive comparison line from Ca XVI is detectable. The Ca XV line flux ratio, $F(2p^2$ $^3P_2$ − $2p3d$ $^3D_3)/F(2p^2$ $^3P_0$ − $2p3d$ $^3D_1)$ is used to estimate flare electron densities at ~4×10^6 K. The derived densities are in rough agreement with those derived from O VII line ratios at ~2×10^6 K. The coronal abundances of Cr and Ca with respect to O are estimated; we find $A(Cr)/A(O) = 0.0036 \pm 0.0018$ and $A(Ca)/A(O) = 0.015 \pm 0.005$. We discuss the determination of these and other abundances by the analysis of X-ray spectra.

PREFACE

We benefitted from discussions of the atomic physics and spectroscopy by Drs. Uri Feldman and Deborah K. Watson.

1

CONTENTS

FIGURES

TABLES

I. INTRODUCTION

X-ray spectra provide a valuable diagnostic tool for the analysis of solar coronal active region plasmas both during and in the absence of flares. Line emission from Fe XVII - Fe XXIV in the wavelength range ~ 10-15 Å provides temperature diagnostics for temperatures, T, in the range ~ 4-20 x 10^6 K (McKenzie and Landecker 1981). With additional information from the lines of Fe XXV around 1.9 Å, the entire range of temperatures above ~ 4 x 10^6 K can be analyzed with lines from a single element for even the most intense flares (Doschek et al. 1980).

For the commonly occurring coronal temperatures 1.5-3 x 10^6 K the Fe X-ray lines are weak, and it is necessary to look to other elements for temperature diagnostics. The strongest lines are the 18.97 Å O VIII 1s $^2S_{1/2}$ - 2p $^2P_{1/2,3/2}$ line (maximum emission at ~ 3 x 10^6K) and the 21.60 Å O VII 1s^2 $^1S_0$ - 1s2p $^1P_1$ line (~ 2 x 10^6 K). The lines of O VII also provide a useful density diagnostic at 2 x 10^6 K (Gabriel and Jordan 1969; McKenzie et al. 1980a). Unfortunately, there are difficulties in the use of the O VII and O VIII lines for temperature diagnostics. First, the coronal O/Fe abundance ratio is poorly known. Withbroe (1976) tabulates observational ratios ranging from 4.6-27 and arrives at 8.1 as his best estimate. Furthermore, we found (McKenzie and Landecker 1981) that our observations could be fitted with any O/Fe in the range 5-10. This abundance uncertainty led to a large uncertainty in the differential emission measure function below ~ 4 x 10^6 K. The second problem is that the lines of O VII, O VIII, and Fe XVII all have large values of $\Delta T/T_{max}$, where

7

T_{max} is the temperature of maximum emissivity and ΔT is the full width at half—maximum (FWHM) of the emissivity function. This subjects the derivation of differential emission measure, the necessary first step in analyzing the coronal plasma, to large uncertainties (Craig and Brown 1976) and accounts for much of the difficulty in deriving the O/Fe abundance ratio from X-ray observations.

This paper treats the coronal X-ray spectrum at wavelengths longer than 15 Å. At shorter wavelengths the spectrum is dominated by Fe and is very dense with lines during flares (McKenzie et al. 1980b). The long wavelength spectrum (> 15 Å) includes relatively weak lines from N, Ca, and Cr, in addition to the strong lines of O VII, O VIII, Fe XVII, and Fe XVIII. The line spectra will permit us to estimate the coronal abundances of Cr and Ca. The N/O abundance ratio was treated in an earlier paper (McKenzie et al. 1978). Lines from Cr XV, Cr XVI, and Ca XVI should be useful solar flare temperature diagnostics in the range 2-5 x 10^6 K and may also be useful for analysis of strongly emitting nonflaring active regions.

II. SPECTRA

a) Method

The spectra were obtained by the SOLEX B Bragg crystal spectrometer aboard the USAF P78-1 satellite. The spectrometer used an RAP (rubidium acid phthalate; 2d = 26.12 Å) crystal scanning in Bragg angle at a rate of 0.262° s^{-1} in 30.2" steps. SOLEX B has a 60" x 60" (FWHM) multigrid collimator and a filtered channel electron multiplier

8

array (microchannel plate) detector. The SOLEX B spectrometer is described in detail by Landecker, McKenzie, and Rugge (1979) and McKenzie et al. (1980b), and the detector and its calibration by Eng and Landecker (1981).

The weaker X-ray lines to be discussed below were initially found in solar flare spectra. Counts from a number of successive spectral scans were summed for improved statistics. A flare at ~ 2330 UT on 1979 March 31 provided data in the range 7.8-23.0 Å. The summed spectrum from 15.4 to 21.6 Å for this flare is shown in Figure 1. A second flare at ~ 0715 UT on 1980 May 9, more intense than the March 31 event, provided data in the range 18.4-23.0 Å. In addition, ~ 20 nonflaring active region observations (7.8-23.0 Å) made during 1979 March-July were used in the analysis. These latter spectra revealed the low-temperature behavior of the lines, thereby aiding in identification, and provided the data used for the Cr abundance determination.

Table 1 lists the spectral lines observed in the two flares discussed above. The wavelength range shortward of 18.4 Å was not scanned in the 1980 May 9 flare, and a few lines were observed only in this flare and not in the less intense 1979 March 31 event. Each line's flux is given for each of the two flares; the spectra are time-integrated over the onset, peak, and decay phases of the flares. The fluxes were computed by using a profile-fitting computer program that included a correction for background. Where necessary, detector dead time corrections were made on the individual spectra before summing. In some cases the two flare spectra yielded slightly different wavelengths. The wavelengths given in the table are our best estimates
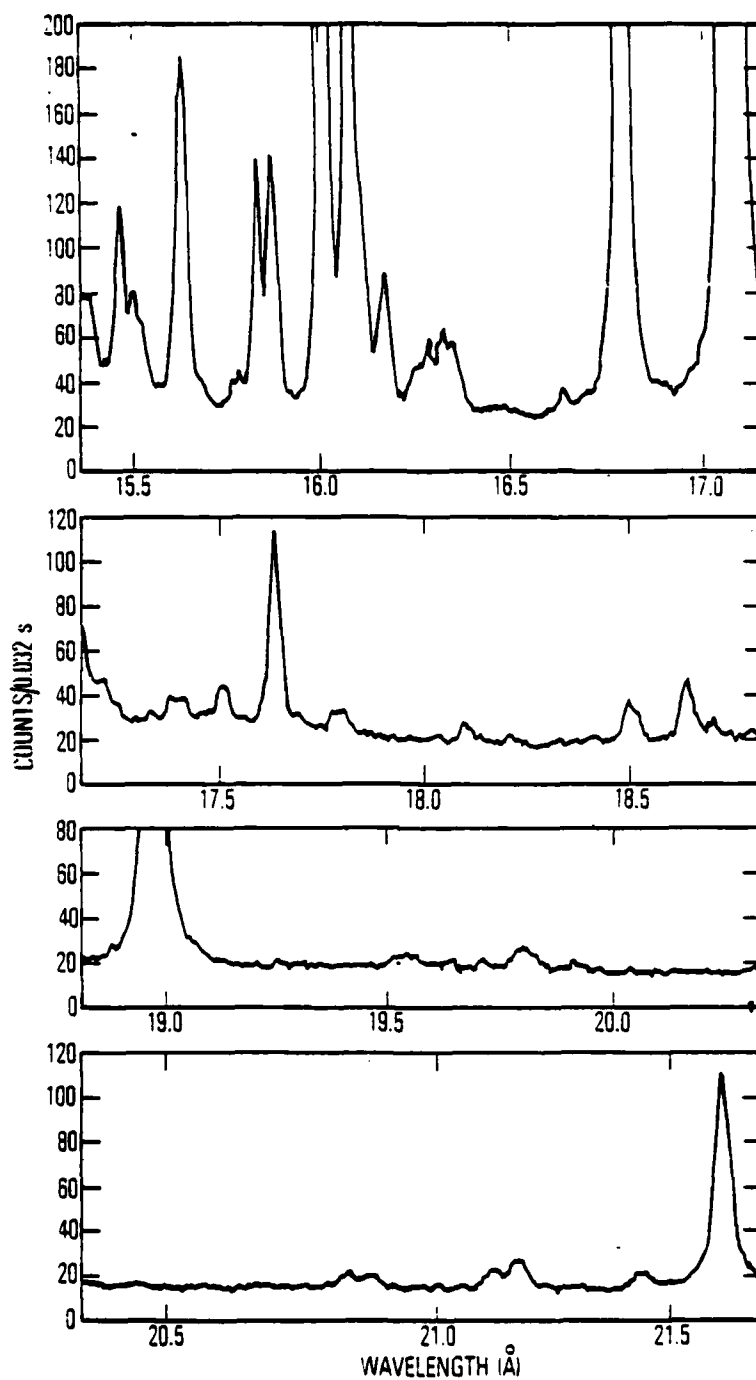
Fig. 1. The Solar X-Ray Spectrum 15.4 to
21.7 Å for a Flare on 1979 March 31.
Data are averaged over 13 successive
wavelength scans spanning ~2200 s.
Table 1 gives fluxes for all of the lines.

TABLE 1
Spectral Lines

Wavelength (Å)		Species	Transition	Flux (10^6 cm^{-2} s^{-1})	
Observed	Reference			79-3-31	80-5-9
15.458	15.455	Fe XVII	$2p^6\,{}^1S_0 - 2p^5 3d\,{}^3P_1$	0.129	
15.496	15.491	Fe XVIII	$2p^5\,{}^2P_{1/2} - 2p^4({}^1S)3s\,{}^2S_{1/2}$	0.050	
15.519*	15.520	Cr XVIII	$2p^3\,{}^4S_{3/2} - 2p^2({}^3P)3d\,{}^4P_{5/2}$	0.034	
	15.512	Cr XVIII	$2p^3\,{}^4S_{3/2} - 2p^2({}^3P)3d\,{}^4P_{3/2}$		
15.632	15.623	Fe XVIII	$2p^5\,{}^2P_{3/2} - 2p^4({}^1D)3s\,{}^2D_{5/2}$	0.222	
15.769	15.764	Fe XVIII	$2p^5\,{}^2P_{3/2} - 2p^4({}^3P)3s\,{}^2P_{1/2}$	0.020	
15.828	15.826	Fe XVIII	$2p^5\,{}^2P_{3/2} - 2p^4({}^3P)3s\,{}^2P_{3/2}$	0.131	
15.868	15.869	Fe XVIII	$2p^5\,{}^2P_{1/2} - 2p^4({}^1D)3s\,{}^2D_{3/2}$	0.167	
16.005	16.006	O VIII	$1s\,{}^2S_{1/2} - 3p\,{}^2P_{1/2,\,3/2}$	0.480	
16.074	16.073	Fe XVIII	$2p^5\,{}^2P_{3/2} - 2p^4({}^3P)3s\,{}^4P_{5/2}$	0.509	
16.110	16.109	Fe XVIII	$2p^5\,{}^2P_{1/2} - 2p^4({}^3P)3s\,{}^4P_{1/2}$	0.117	
16.170*	16.17	Fe XVIII	$2s2p^6\,{}^2S_{1/2} - 2s2p^5 3s\,{}^2P_{3/2}$	0.104	
16.249*	16.249	Cr XVII	$2p^4\,{}^3P_1 - 2p^3({}^2P)3d\,{}^3D_2$ (?)	0.025	
16.279	16.270	Fe XVIII	$2p^5\,{}^2P_{1/2} - 2p^4({}^3P)3s\,{}^4P_{3/2}$	0.043	
16.319*	16.311	Cr XVII	$2p^4\,{}^3P_2 - 2p^3({}^2P)3d\,{}^3P_2$ (?)	0.054	
16.344	16.348	Fe XVIII	$2p^5\,{}^2P_{1/2} - 2p^4({}^3P)3s\,{}^4P_{5/2}$	0.046	
16.633*	16.640	Cr XVII	$2p^4\,{}^3P_1 - 2p^3({}^2D)3d\,{}^3D_2$ (?)	0.010	
16.787	16.775	Fe XVII	$2p^6\,{}^1S_0 - 2p^5 3s\,{}^1P_1$	1.47	
17.054	17.051	Fe XVII	$2p^6\,{}^1S_0 - 2p^5 3s\,{}^3P_1$	1.84	
17.098	17.097	Fe XVII	$2p^6\,{}^1S_0 - 2p^5 3s\,{}^3P_2$	1.82	

*See discussion in text

11

TABLE 1 (Con't)
Spectral Lines

Wavelength (Å) Observed	Reference	Species	Transition	Flux $(10^6 \text{ cm}^{-2}\text{ s}^{-1})$ 79-3-31	80-5-9
17.201*	17.199	Fe XVI	$2p^6 3p\ ^2P_{3/2} - 2p^5 3s 3p\ ^2D_{5/2}$		
	17.206	Fe XVI	$2p^6 3p\ ^2P_{1/2} - 2p^5 3s 3p\ ^4D_{3/2}$	0.008	
	17.194	Fe XVI	$2p^6 3p\ ^2P_{1/2} - 2p^5 3s 3p\ ^4P_{1/2}$		
17.318				0.006	
17.367*	17.370	Cr XVI	$2p^5\ ^2P_{3/2} - 2p^4(^1D)3d\ ^2D_{5/2}$	0.021	
17.400*	17.396	O VII	$1s^2\ ^1S_0 - 1s5p\ ^1P_1$	0.023	
17.501*	17.497	Fe XVI	$2p^6 3p\ ^2P_{3/2} - 2p^5 3s 3p\ ^2D_{3/2}$		
	17.498	Fe XVI	$2p^6 3p\ ^2P_{3/2} - 2p^5 3s 3p\ ^4P_{5/2}$	0.032	
	17.509	Fe XVI	$2p^6 3p\ ^2P_{1/2} - 2p^5 3s 3p\ ^4P_{3/2}$		
	17.496	Fe XVI	$2p^6 3d\ ^2D_{5/2} - 2p^5 3s 3d\ ^4P_{5/2}$		
17.626*				0.201	
17.684				0.005	
17.770	17.768	O VII	$1s^2\ ^1S_0 - 1s4p\ ^1P_1$	0.016	
17.798	17.793	Cr XVI	$2p^5\ ^2P_{3/2} - 2p^4(^3P)3d\ ^4P_{3/2}$	0.020	
18.090				0.022	
18.202				0.005	
18.401				0.003	
18.497	18.497	Cr XV	$2p^6\ ^1S_0 - 2p^5 3d\ ^1P_1$	0.061	0.175
18.565					0.026
18.624	18.627	O VII	$1s^2\ ^1S_0 - 1s3p\ ^1P_1$	0.073	0.244
18.689	18.692	Ca XVIII	$2s\ ^2S_{1/2} - 3p\ ^2P_{3/2}$	0.021	0.136

*See discussion in text

TABLE 1 (Con't)

Spectral Lines

Wavelength (Å)		Species	Transition	Flux $(10^6\ cm^{-2}\ s^{-1})$	
Observed	Reference			79-3-31	80-5-9
18.733	18.734	Ca XVIII	$2s\ ^2S_{1/2} - 3p\ ^2P_{1/2}$		0.076
18.783	18.782	Cr XV	$2p^6\ ^1S_0 - 2p^5 3d\ ^3D_1$		0.057
18.969	18.969	O VIII	$1s\ ^2S_{1/2} - 2p\ ^2P_{1/2,\ 3/2}$	1.75	5.67
19.261	19.255	Cr XVI	$2p^5\ ^2P_{3/2} - 2p^4(^1D)3s\ ^2D_{5/2}$		0.049
19.300					0.048
19.511	19.511	Cr XVI	$2p^5\ ^2P_{3/2} - 2p^4(^1D)3s\ ^2D_{3/2}$	0.009	
19.532	19.538	Cr XVI	$2p^5\ ^2P_{3/2} - 2p^4(^3P)3s\ ^2P_{3/2}$	0.015	0.050
19.564	19.562	Ca XVII	$2s^2\ ^1S_0 - 2s3p\ ^1P_1$	0.017	0.048
19.640	19.643	Ca XVIII	$2p\ ^2P_{1/2} - 3d\ ^2D_{3/2}$	0.012	0.056
19.715	19.714	Cr XVI Cr XVI	$2p^5\ ^2P_{1/2} - 2p^4(^3P)3s\ ^2P_{1/2}$ $2p^5\ ^2P_{3/2} - 2p^4(^3P)3s\ ^4P_{3/2}$	0.007	0.019
19.788	19.790	Ca XVIII	$2p\ ^2P_{3/2} - 3d\ ^2D_{5/2}$	0.044	0.118
19.808	19.807	Cr XVI Cr XVI	$2p^5\ ^2P_{3/2} - 2p^4(^3P)3s\ ^4P_{5/2}$ $2p^5\ ^2P_{1/2} - 2p^4(^3P)3s\ ^2P_{3/2}$		0.060
19.916				0.015	0.039
20.126					0.028
20.288					0.066
20.316	20.326	Ca XVII	$2s2p\ ^3P_1 - 2s3d\ ^3D_2$		0.032
20.434	20.436	Ca XVII	$2s2p\ ^3P_2 - 2s3d\ ^3D_3$		0.032
20.863	20.863	Cr XV	$2p^6\ ^1S_0 - 2p^5 3s\ ^1P_1$	0.071	0.140
20.913	20.910	N VII	$1s\ ^2S_{1/2} - 3p\ ^2P_{1/2,\ 3/2}$	0.055	0.152

*See discussion in text

TABLE 1 (Con't)
Spectral Lines

Wavelength (Å)		Species	Transition	Flux $(10^6 \ cm^{-2} \ s^{-1})$	
Observed	Reference			79-3-31	80-5-9
21.156	21.153	Cr XV	$2p^6 \ ^1S_0 - 2p^5 3s \ ^3P_1$	0.078	0.126
21.204	21.208	Cr XV	$2p^6 \ ^1S_0 - 2p^5 3s \ ^3P_2$	0.150	0.336
	21.193	Ca XVII	$2s2p \ ^1P_1 - 2s3d \ ^1D_2$		
21.444	21.450	Ca XVI	$2p \ ^2P_{1/2} - 3d \ ^2D_{3/2}$	0.067	0.140
21.601	21.601	O VII	$1s^2 \ ^1S_0 - 1s2p \ ^1P_1$	1.30	3.00
21.807	21.804	O VII	$1s^2 \ ^1S_0 - 1s2p \ ^3P_1$	0.383	1.96
22.025				0.018	0.138
22.100	22.098	O VII	$1s^2 \ ^1S_0 - 1s2s \ ^3S_1$	0.920	0.862
22.733	22.732	Ca XV	$2p^2 \ ^3P_0 - 2p3d \ ^3D_1$	0.225	0.276
22.778	22.779	Ca XV	$2p^2 \ ^3P_2 - 2p3d \ ^3D_3$	0.065	0.243

*See discussion in text

from the available data. In all cases, the wavelengths were assigned through the use of a scale based on a prelaunch calibration which was adjusted for each flare with benchmark wavelengths from three lines: Fe XVII $2p^6$ $^1S_0$ - $2p^53d$ $^1P_1$ (15.013 Å), O VIII 1s $^2S_{1/2}$ - 2p $^2P_{1/2,3/2}$ (18.969 Å), and O VII $1s^2$ $^1S_0$ - 1s2p $^1P_1$ (21.601 Å). The tabulated reference wavelengths were mostly taken from a small number of publications: Feldman et al. (1973; Fe XVIII, Cr XVI), Hutcheon, Pye, and Evans (1976; Fe XVII), Ermolaev and Jones (1973; O VII), Garcia and Mack (1965; O VIII, N VII), Sugar and Corliss (1977; Cr), and Sugar and Corliss (1979; Ca). In the case of blends in Fe XVIII, the dominant line according to the calculations of Cowan (1973) is cited. We estimate that the wavelength accuracy is typically better than 10 mÅ. This is somewhat better than the reported accuracy for spectra of a flare on 1979 June 10 (McKenzie et al. 1980b). The improvement is attributable to the exclusion in the present spectra of lines shortward of 15 Å, where the spectrometer has relatively low dispersion, and to the reading out of data every step instead of every other step as was done in the earlier case.

b) Discussion of Selected Line Identifications

A number of lines in the table, those denoted by asterisks, require further discussion or clarification. The following paragraphs provide that discussion.

The line at 15.519 Å is identified as a blend of Cr XVIII lines, $2p^3$ $^4S_{3/2}$ - $2p^2(^3P)3d$ $^4P_{5/2,3/2}$ (Fawcett and Hayes 1975). A similar blend at around 12.83 Å in Fe XX had about one-third the strength of

15

the Fe XVII $2p^6$ $^1S_0$ - $2p^53d$ $^1P_1$ line during the hot rise phase of the flare of 1979 June 10 (McKenzie et al. 1980b). In Cr the same ratio was ~ 0.55 in the 1979 March 31 flare (see § IIc for a discussion of the Cr lines).

The identification of the line at 16.170 Å as Fe XVIII $2s2p^6$ $^2S_{1/2}$ - $2s2p^53s$ $^2P_{3/2}$ is based upon Cohen, Feldman, and Kastner (1968). The line is not discussed by Feldman et al. (1973), and it was observed but not identified in a laser-produced Fe spectrum by Bromage et al. (1977). The line is of such strength that we consider that it must arise from Fe XVII or Fe XVIII (taking its wavelength into consideration). Interestingly, Loulergue and Nussbaumer (1975) list the Fe XVII $2p^53p$ $^1P_1$ level at 6187605 cm^{-1}, so that a transition to the ground level $2p^6$ $^1S_0$ would have a wavelength of 16.161 Å. By solving the level population equations for Fe XVII using data from Loulergue and Nussbaumer (1975), we estimate that A($2p^53p$ $^1P_1$ - $2p^6$ $^1S_0$) would have to be ~ 10^{10} to account for the observed line flux. This is high for a magnetic dipole transition. Further, some of the Loulergue and Nussbaumer (1975) level energies are inaccurate. Therefore, we prefer the Fe XVIII line identification.

The three unidentified lines at 16.249, 16.319, and 16.633 Å may arise from Cr XVII, but the strengths of the lines raise difficulties with the identifications. The strongest Cr XVII line is expected to be $2p^4$ $^3P_2$ - $2p^3(^2D)3d$ $^3D_3$, based on calculations by Bromage and Fawcett (1977) and observations by Fawcett and Hayes (1975). This is the strongest line from the isoelectronic species, Fe XIX, and spin-orbit interactions cause only minor changes in the level composition

between Cr XVII and Fe XIX (Bromage and Fawcett 1977). We find no line at 16.46 Å, the expected Cr XVII wavelength (Fawcett and Hayes 1975). For this reason we cannot identify the lines at 16.249, 16.319, and 16.633 Å with confidence.

The lines at 17.201 and 17.501 Å are identified by Burkhalter et al. (1979) as blends of Fe XVI satellite lines. We have listed the lines in LS notation for the sake of consistency, although Burkhalter et al. warn that LS coupling is a poor approximation for these lines. Fe XVI lines may be blended with the lines at 17.367 and 17.400 Å in the table. This might account for the observed flux of O VII $1s^2\ ^1S_0 - 1s5p\ ^1P_1$ appearing to exceed that of O VII $1s^2\ ^1S_0 - 1s4p\ ^1P_1$. The lines at 17.201 Å may be blended with the O VII $1s^2\ ^1S_0 - 1s6p\ ^1P_1$ line (Kelly and Palumbo 1973).

McKenzie et al. (1980b) tentatively identified a line at 17.617 Å as the Fe Lα characteristic X-ray. The current spectrum has a strong line at 17.626 Å, which is considerably above laboratory values for Fe Lα of 17.59 Å (Bearden 1967). Furthermore, rough calculations of the production of Fe Lα by fluorescence fall far short of the observed fluxes. These observations cast doubt on the earlier identification.

c) Lines from Highly Ionized Chromium

In this section we present the evidence supporting the detection of Cr X-ray emission in the solar corona. Comparisons between the Cr and Fe spectra and the few available theoretical calculations will be used. We conclude the section by estimating the Fe/Cr and O/Cr abundance ratios.

i) Line Identifications

The lines of Cr XV are expected to be relatively strong since those of Fe XVII, also neon-like, are strong in both flare and active-region spectra. The Cr XV $2p^6$ $^1S_0$ - $2p^53d$ $^1P_1$ line at 18.497 Å is prominent in our spectra. The low second-order reflectivity of the RAP crystal (Burek 1976) assures that this line contains no second-order Mg XI radiation. We show below that the relative fluxes of the Cr XV lines agree well with theoretical expectations. This shows that undetected blends are unlikely to change the measured flux of the $2p^6$ $^1S_0$ - $2p^53d$ $^1P_1$ line substantially.

The most prominent Fe XVII lines are, in order of decreasing strength, the transitions to the ground state from the $2p^53d$ $^1P_1$, $2p^53s$ $^3P_1$, $2p^53s$ $^3P_2$, $2p^53s$ $^1P_1$, and $2p^53d$ $^3D_1$ levels. Line radiation from each of these transitions in Cr XV is detectable in the 1980 May 9 flare spectrum. All except the $^3D_1$ line are apparent in Figure 1. Figure 2 shows both of the 3d lines in the May 9 flare. The 3d $^3D_1$ line falls in the "valley" between the Ca XVIII and O VIII lines and therefore appears to be weak. We find that the $^3D_1/^1P_1$ line ratio is 0.33. Loulergue and Nussbaumer's (1975) calculations give 0.37 for the same ratio in Fe XVII and 0.42 in Ni XIX, so 0.33 would probably agree well with theory for Cr XV.

The Cr XV lines with the upper level configuration $2p^53s$ are apparent in Figure 1. The strengths of the $^3P_1$ (21.153 Å) and $^1P_1$ (20.863 Å) lines are approximately equal to that of the 3d $^1P_1$ line. This is what we expect, judging from the Loulergue and Nussbaumer
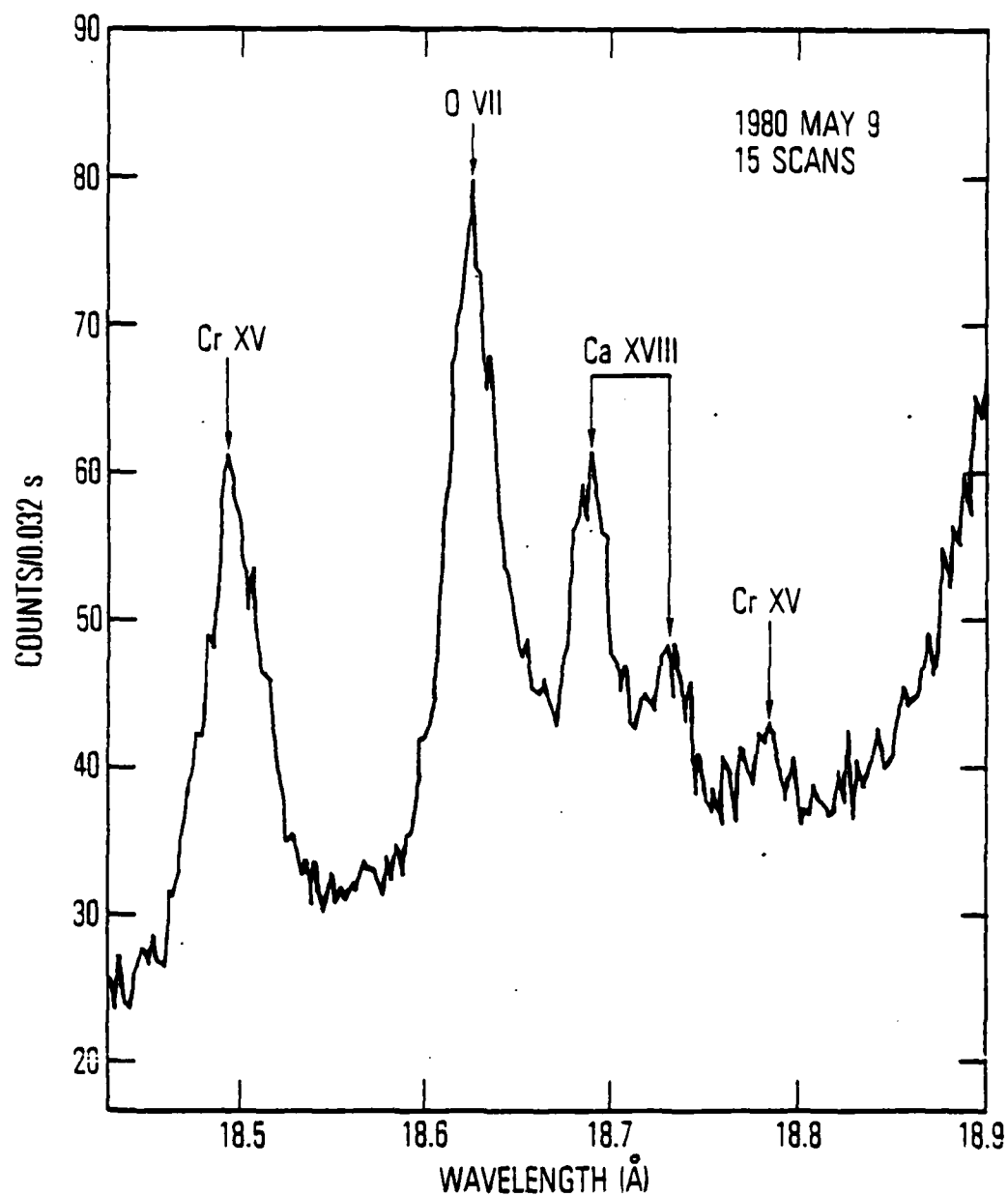
Fig. 2. Part of the 1980 May 9 Flare X-Ray Spectrum. The lines shown are; Cr XV $2p^6$ $^1S_0$ – $2p^53d$ $^1P_1$, O VII $1s^2$ $^1S_0$ – $1s3p$ $^1P_1$, Ca XVIII $2s$ $^2S_{1/2}$ – $3p$ $^2P_{3/2,1/2}$, and Cr XV $2p^6$ $^1S_0$ – $2p^53d$ $^3D_1$. Data are averaged over 15 successive wavelength scans spanning ~960 s.

19

(1975) calculations. Because the $2p^5 3s$ levels of the neon-like ions are primarily excited by cascade, a calculation involving many levels, transitions, and collision rates must be made to predict the spectrum. Since the data for such a calculation are unavailable for Cr XV, line ratios can only be roughly predicted. The $^3P_2$ line, for which we calculate $\lambda = 21.208$ Å, is blended with Ca XVII $2s2p$ $^1P_1$ – $2s3d$ $^1D_2$. In § IId we discuss this blend and conclude that the $^3P_1$ and the $^3P_2$ lines have approximately equal flux. This agrees well with the expected strength of the $^3P_2$ line. In summary, the five Cr XV lines expected to be strongest are all observed in our spectra, and their relative fluxes are approximately as expected. This is very good evidence in support of the Cr XV line identifications.

The Cr XVI spectrum corresponds well to that of Fe XVIII. Of the seven brightest Fe XVIII lines listed by McKenzie et al. (1980b), Cr XVI lines for six are in Table 1. The exception is $2p^5$ $^2P_{3/2}$ – $2p^4(^3P)3d$ $^2D_{5/2}$ which is expected in Cr XVI at 17.603 Å (Feldman et al. 1973) and is thus swamped by the strong line at 17.626 Å. Table 1 also includes the Cr XVI $2p^5$ $^2P_{3/2}$ – $2p^4(^3P)3s$ $^4P_{3/2}$ line (19.714 Å). The corresponding Fe XVIII line, at 16.003 Å, is blended with a strong O VIII line.

In addition to lines from Cr XV and XVI, Table 1 contains a blend attributed to Cr XVIII. The Cr XVII spectrum was discussed previously. The radiation from more highly stripped Cr species is at wavelengths below 15 Å (Fawcett and Hayes 1975) where strong Fe lines dominate the spectrum.

ii) The Coronal Abundance of Chromium

Having established the identity of a large number of Cr lines in the solar spectrum, we can now make an estimate of the coronal Cr abundance. The power emitted in the spectral line $j \to i$, excited by collisions from the ground state is

$$P_{ji} = 8.63 \times 10^{-6} \frac{A_H A_Z h \nu B_{ji}}{2J_g + 1} \int \frac{\epsilon(T) a_z(T) \Omega_{gj}(T) \exp(-E_{gj}/kT) dT}{T^{1/2}} \text{ erg s}^{-1}, \quad (1)$$

where A_H is the number of hydrogen nuclei per electron in the plasma, A_Z the element abundance, $h\nu$ the X-ray energy, B_{ji} the branching ratio, J_g the ground state angular momentum, $a_z(T)$ the fractional population of ion stage z, $\Omega_{gj}(T)$ the temperature-averaged collision strength, E_{gj} the energy of state j, and T the temperature. The differential emission measure, $n_e^2 \frac{dV}{dT}$, where n_e is the electron density and V the volume, is $\epsilon(T)$. Equation (1) holds, provided level j is populated from the ground state by collisions and depopulates radiatively. For Cr XV cascade is an important population mechanism, but it is small for the $2p^5 3d \; ^1P_1$ level, so the equation is valid for the line at 18.497 Å. We will determine the O/Cr and Fe/Cr abundance ratios with equation (1) by using the O VIII $1s \; ^2S - 2p \; ^2P$ line and the Fe XVII $2p^6 \; ^1S_0 - 2p^5 3d \; ^1P_1$ line.

To determine the Cr abundance we need to know the atomic physics parameters B_{ji}, $a_z(T)$, and $\Omega_{gj}(T)$. The first is easily obtained for the lines under consideration, but $a_z(T)$ and $\Omega_{gj}(T)$ are not readily available for Cr. Landini and Fossi (1972) calculated the ionization balance for Cr, but those calculations are probably obsolete in view

21

of more sophisticated techniques currently in use. We estimated $a_z(T)$ for Cr XV by interpolating between the calculations for the neon-like species Ca XI (Jacobs et al. 1980) and Fe XVII (Jacobs et al. 1977). For $\Omega_{gj}(T)$ we followed the procedure adopted by Loulergue and Nussbaumer (1975), setting

$$\Omega_{gj}(Cr\ XV) = \left(\frac{17}{15}\right)^2 \Omega_{gj}(Fe\ XVII). \tag{2}$$

The Fe XVII collision strength was taken from Merts et al. (1980), and that of O VIII from Magee et al. (1977). Figure 3 shows the normalized emissivities of the three lines under discussion here and two additional lines to be used below.

The integral in equation (1) must be evaluated to determine the line flux. We assumed the following form for the differential emission measure:

$$\epsilon(T) = \begin{cases} a\ T^b & T < T_{max} \\ 0 & T > T_{max} \end{cases} \tag{3}$$

In Equation (3) a and b are constants, and b can be positive or negative. For active region observations we took $T_{max} = 8\times10^6$ K. We determined b by evaluating equation (1) for O VII $1s^2\ ^1S_0 - 1s3p\ ^1P_1$ and O VIII 1s $^2S - 2p\ ^2P$ and comparing calculated and observed line ratios. These two lines were chosen because they are from the same element and have nearly equal wavelengths so that uncertainties in the instrumental sensitivity are minimized. These lines also effectively cover the temperature range in which the lines of interest are primarily produced.

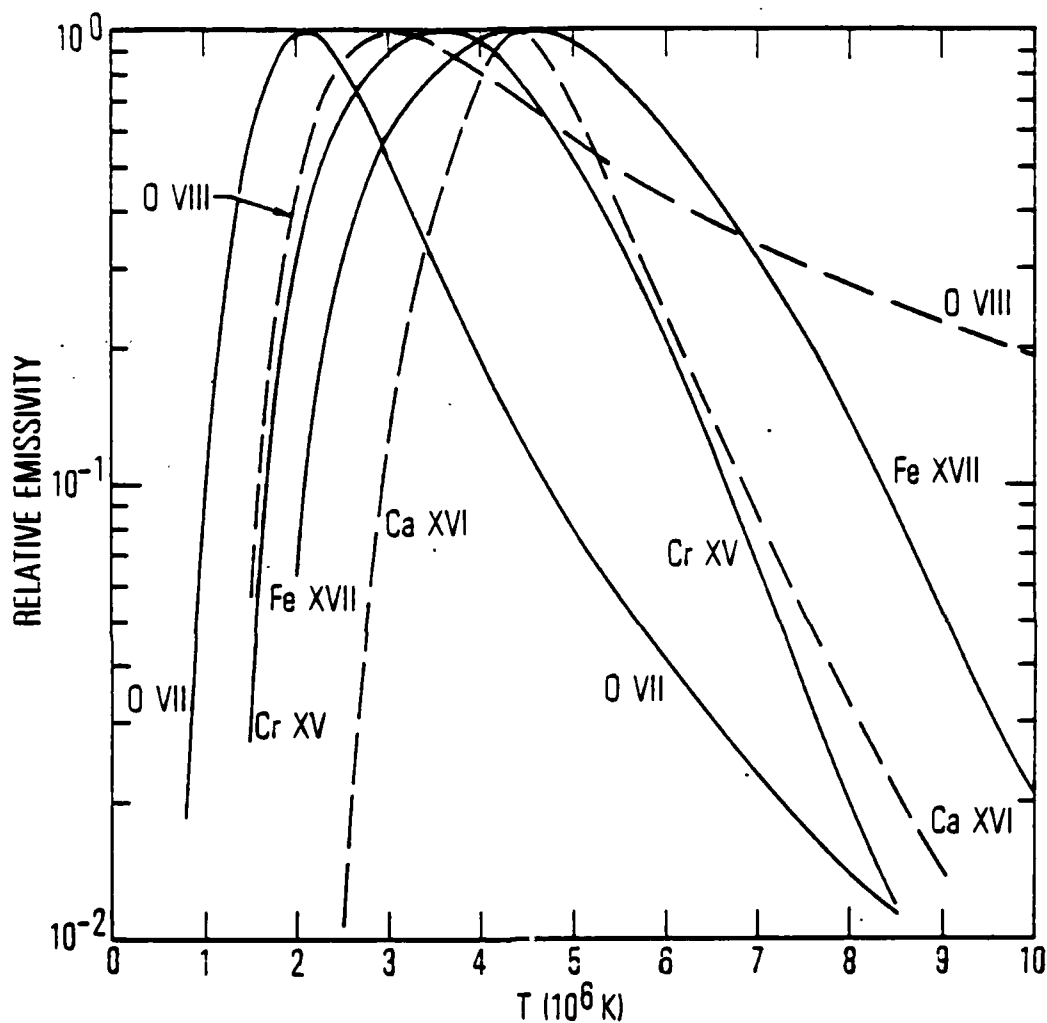Fig. 3. Relative Emissivity as a Function of Temperature for the
Following Spectral Lines: O VII $1s^2\ ^1S_0 - 1s2p\ ^1P_1$
(21.601 Å), O VIII $1s\ ^2S - 2p\ ^2P$ (18.969 Å), Cr XV
$2p^6\ ^1S_0 - 2p^53d\ ^1P_1$ (18.497 Å), Fe XVII $2p^6\ ^1S_0 - 2p^53d\ ^1P_1$
(15.013 Å), and Ca XVI $2p\ ^2P_{1/2} - 3d\ ^2D_{3/2}$ (21.444 Å). Each
curve is normalized so that the maximum emissivity is unity.

23

The Cr abundance determinations were made by using spectra from nonflaring active regions. Data were summed over ~ 10 consecutive wavelength scans (~ 1700 s) for improved statistics. Nonflare spectra were used because they constitute a reasonably large data base for which accurate line fluxes were easier to derive than in flare spectra.

Fourteen summed spectra were available for the O/Cr abundance determination. The accuracy of this determination should be limited primarily by the approximations used in deriving the atomic physics data for Cr. The O VIII and Cr XV lines used are close in wavelength so that instrumental uncertainties are small. Furthermore the O VIII emissivity curve is similar to that of Cr XV except at high temperatures for which $\epsilon(T)$ is expected to be small in the nonflaring corona. Thus the flux ratio should depend weakly on the form of $\epsilon(T)$. This was indeed the case as we found, typically, $b \approx -1$. Weighting the individual determinations by σ^{-2}, where σ is the estimated statistical standard deviation, we found $A(O)/A(Cr) = 277 \pm 26$, where we quote a 90% confidence interval. For Fe and Cr, 12 observations gave $A(Fe)/A(Cr) = 37 \pm 4$. The error estimates include statistical uncertainties only, so they are understated. The atomic parameters for Cr are uncertain, and instrumental uncertainties are not negligible for $A(Fe)/A(Cr)$. Combining all of these considerations, we estimate $A(O)/A(Cr) = 277 \pm 140$ and $A(Fe)/A(Cr) = 37 \pm 18$.

d) Lines from Highly Ionized Calcium

i) Line Identifications

Table 1 includes the lines expected to be strongest for each species Ca XV - Ca XVIII. McKenzie et al. (1980b) list six lines from Fe XXIV. Of these, four are found in Table 1 for Ca XVIII, the exceptions being $2p\ ^2P_{1/2,3/2} - 3s\ ^2S_{1/2}$, which are expected at 20.052 Å and 20.218 Å, respectively (Sugar and Corliss 1979). The $2p\ ^2P_{3/2} - 3d\ ^2D_{5/2}$ line (19.788 Å) is blended with Cr XVI lines in both spectra, but the 1980 May 9 spectrum was sufficiently strong to allow the fitting program to estimate the Ca XVIII flux. The relative line strengths for Ca XVIII are approximately the same as in Fe XXIV (McKenzie et al. 1980b), except that the $2p\ ^2P_{1/2} - 3d\ ^2D_{3/2}$ line is apparently weak in Ca. This apparent weakness might be attributable to blending in the Fe spectrum.

The three Ca XVII lines at 20.316, 20.434, and 21.193 Å are identified based upon Fawcett and Hayes (1975); the reference wavelengths are their calculated values. The Ca XVII, $2s2p\ ^1P_1 - 2s3d\ ^1D_2$ line at 21.193 Å is blended with the Cr XV $2p^6\ ^1S_0 - 2p^53s\ ^3P_2$ line at 21.208 Å so that the combination has roughly twice the intensity of the Cr XV $2p^6\ ^1S_0 - 2p^53s\ ^3P_1$ line. On the basis of reported Fe XVII and Ni XIX calculations and observations (Loulergue and Nussbaumer 1975 and references therein) as well as our own observations of Fe XVII lines (McKenzie et al. 1980b and Table 1, above), we expect the $^3P_1$ line to be slightly stronger than the $^3P_2$. Nonflaring active region spectra, which arise from lower temperature plasmas where

Ca XVII emission is weak compared to that of Cr XV, show that the flux at 21.156 Å is approximately equal to that at 21.204 Å. Therefore, we estimate that half or more of the 21.204 Å emission arises from Ca XVII.

The foregoing discussion implies that $2s2p$ $^1P_1$ - $2s3d$ $^1D_2$ is by far the strongest Ca XVII X-ray line. The same conclusion holds for the isoelectronic species, Fe XXIII. McKenzie et al. (1980b) reported, but did not identify, a strong line at 11.742 Å. Examination of our 1979 March 31 spectra indicate that this line arises from an ion at least as highly stripped as Fe XXII. Fawcett and Hayes (1975) calculated a wavelength of 11.74 Å for Fe XXIII $2s2p$ $^1P_1$ - $2s3d$ $^1D_2$, and recent calculations by Bhatia and Mason (1981) indicate that this should be, as it is in our spectra, the strongest Fe XXIII line. Finally, there is weak evidence for the $2s2p$ $^3P_2$ - $2s3d$ $^3D_3$ line in Fe XXIII, but the $2s2p$ $^3P_1$ - $2s3d$ $^3D_2$ line has not been detected in our spectra.

The only Ca XVI line detected, the $2p$ $^2P_{1/2}$ - $3d$ $^2D_{3/2}$ line at 21.444 Å, corresponds to the strongest Fe XXII line (McKenzie et al. 1980b). The Ca XVI line is discussed in detail below, where we use it to determine the Ca/O abundance ratio.

ii) Density-Sensitive Ca XV Line Ratio

The Ca XV lines are of particular interest because the flux ratio $F(2p^2$ $^3P_2$ - $2p3d$ $^3D_3)/F(2p^2$ $^3P_0$ - $2p3d$ $^3D_1)$ is density-sensitive. The collision strengths, $\Omega(^3P_0$ - $^3D_3)$ and $\Omega(^3P_1$ - $^3D_3)$ are very small

(Mason et al. 1979). Since the $^3P_2$ level population is low except at high densities, the $2p^2$ $^3P_2$ - 2p3d $^3D_3$ line is weak. The $^3P_2$ level population increases with density until it becomes nearly constant. As a result the above flux ratio increases with density and may exceed unity in the high-density limit. The $2p^2$ $^3P_2$ - 2p3d $^3D_3$ line is the strongest of a number of such density-sensitive lines in the carbon-like ions (Mason et al. 1979).

Figure 4 shows the Ca XV spectra for the two flares under discussion and from the nonflaring sun. The upper curve is the sum of 207 individual spectra, giving a total of 6.6 s exposure at each data point. The flare spectra are, as before, summed over all available flare data. Although the spectrometer resolution is poor and the efficiency is low at these long wavelengths, the increasing importance of the longer wavelength component with increasing electron density is apparent. The density in the May 9 flare was much higher than in the March 31 flare (Doschek et al. 1981, McKenzie and Landecker 1981). The $2p^2$ $^3P_1$ - 2p3d $^3D_2$ (22.756 Å) and the $2p^2$ $^3P_1$ - 2p3d $^3D_1$ (22.824 Å) lines are also noted in Figure 4. The former is a density-sensitive line that is weaker than the $^3P_2$ - $^3D_3$ line, and the latter should be present at a constant ratio to the $^3P_0$ - $^3D_1$ line, regardless of density. These lines are not in Table 1 because their detection is marginal.

Mason et al. (1979) have calculated the line strengths for Fe XXI (isoelectronic to Ca XV) as a function of density, and Mason (1975) has calculated the relative populations of the $2p^2$ ^3P levels in Ca XV. With these calculations we can use the Ca XV fluxes to estimate
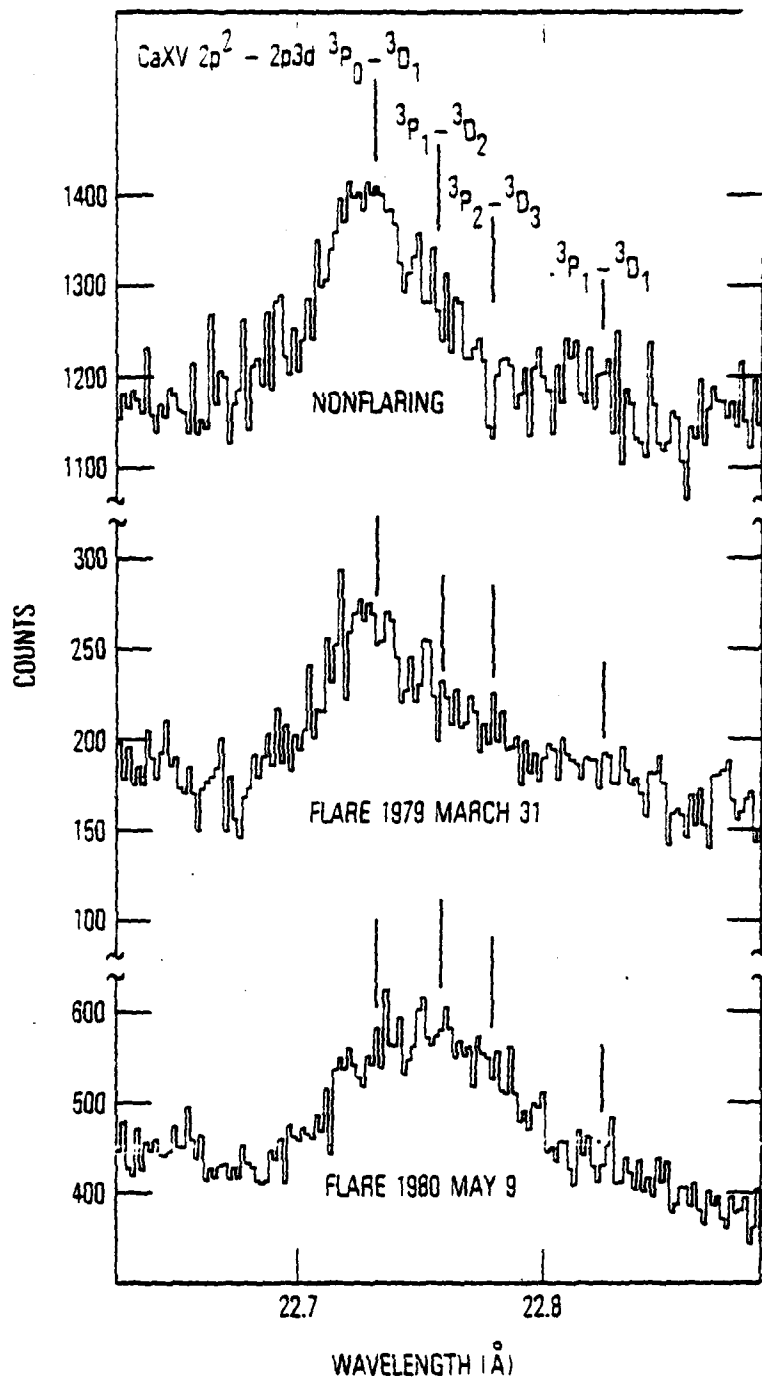
Fig. 4. Ca XV Line Spectra from Two Flares and a Sum Over 207 Nonflare Spectral Scans. The scales are chosen to illustrate the increased $^3P_2 - ^3D_3$ line emission in the two flare spectra. The calculated wavelengths of four lines are marked.

28

electron densities at $\sim 4 \times 10^6$ K. The fitting program was used to estimate line fluxes. The $2p^2\ ^3P_1 - 2p3d\ ^3D_2$ line was included for May 9 but was constrained to have flux equal 0.3 times that of the $^3P_2 - ^3D_3$ line. The line was excluded for the other two, lower-density spectra. The quality of fit obtained was insensitive to the flux of this line, as was the $(^3P_2 - ^3D_3)/(^3P_0 - ^3D_1)$ line ratio. For the 1979 March 31 and 1980 May 9 flares we found $n_e \sim 6 \times 10^{10}$ and 2×10^{11} cm^{-3}, respectively. From an O VII line ratio (T $\approx 2 \times 10^6$ K), we found $n_e \sim 2 \times 10^{10}$ and 2.5×10^{11} cm^{-3} for the two flares. These densities are averaged over all the flare observations, but they indicate that the densities around T $= 4 \times 10^6$ K are comparable to those near 2×10^6 K. The fitting program calculated a $(^3P_2 - ^3D_3)/(^3P_0 - ^3D_1)$ flux ratio of 0.085 for the nonflare spectrum, corresponding to $n_e \sim 10^{10}$ cm^{-3}. This is probably the result of uncertainties in the spectrometer response at long wavelengths and not a real density determination. We have made a search for possible blended lines from species other than Ca XV in all spectral orders up to the fourth and have found no plausible candidates. Thus we believe that the observed line radiation arises exclusively from Ca XV.

iii) The Coronal Abundance of Calcium

The O/Ca abundance ratio is calculated by using the Ca XVI $2p\ ^2P_{1/2} - 3d\ ^2D_{3/2}$ and the O VII $1s^2\ ^1S_0 - 1s2p\ ^1P_1$ lines at 21.444 Å and 21.601 Å, respectively. As was the case for O/Cr, the two lines have similar wavelengths so that calibration uncertainties are minimized. Furthermore the Ca XVI line is the only Ca line for

which we have an expression for the collision strength (Clark and Magee 1981).

Some care must be taken in using the Ca XVI line because it is density-sensitive. The Ca XVI ground term is split with $^2P_{3/2}$ above $^2P_{1/2}$. At high densities the $^2P_{3/2}$ level is populated at the expense of $^2P_{1/2}$, and this changes the excitation of the $^2D_{3/2}$ level. With the calculations of Mason and Storey (1980) for Fe XXII as a guide, we predict that at high densities the Ca XVI line will be weakened. In Fe XXII this effect is about 10% at $n_e = 10^{13}$ cm^{-3}. (The more dramatically density-sensitive 2p $^2P_{3/2}$ - 3d $^2D_{5/2}$ line is at 21.610 Å in Ca XVI and is unobservable because of the strong O VII line.) From the data of Bhatia, Feldman, and Doschek (1980), we calculate that in Ti XVIII the $^2D_{3/2}$ line will be weakened by 10% at a density of $\sim 5\times10^{11}$ cm^{-3}; thus density effects can be expected in Ca XVI for $n_e > 10^{11}$ cm^{-3}. In the 1979 March 31 flare a maximum $n_e \sim 5\times10^{10}$ cm^{-3} was measured at 2×10^6 K by using a ratio of O VII lines (McKenzie and Landecker 1981), while in the 1979 May 9 flare n_e (2×10^6 K) $> 10^{11}$ cm^{-3} throughout the observations reported here (Doschek et al. 1981). Consequently we might expect weakening of the Ca XVI emission in the latter flare but not the former.

The O VII line must also be treated with care. Acton (1978) predicted that the O VII line would be depleted by resonant scattering under certain conditions. In a study in progress we have verified this prediction. The ratio,

$$G = \frac{[F(1s^2\ {}^1S_0 - 1s2p\ {}^3P_1) + F(1s^2\ {}^1S_0 - 1s2s\ {}^3S_1)]}{[F(1s^2\ {}^1S_0 - 1s2p\ {}^1P_1)]}, \qquad (4)$$

where F is flux, is a measure of the effects of resonant scattering. When resonant scattering is absent, $G(1.9 \times 10^6 \text{ K}) \sim 1.0$ (Pradhan and Shull 1981), provided that the plasma is in ionization equilibrium. If $G > 1.0$, a correction for resonant scattering should be made. For the two flares under consideration here, $G \lesssim 1.0$ so no correction was made.

The O/Ca abundance ratio was calculated by the same procedure as was used for the O/Cr ratio. The Ca line is too weak in nonflare spectra, so the two flare spectra were used. Uncertainties in the emission measure are more severe and more important in this case. They are more severe because $b > 0$ and more important because the line emissivities as a function of temperature differ substantially (see Figure 3). We used an upper cut-off of 6×10^6 K because such a cut-off was found in the 1979 March 31 flare (McKenzie and Landecker 1981). For this flare we found $b = 1.5$ and $A(O)/A(Ca) = 79$. For the 1980 May 9 flare $b = 0.7$ and $A(O)/A(Ca) = 57$. We take the difference between these as indicative of the error and set $A(O)/A(Ca) = 68 \pm 22$. We do not estimate $A(Fe)/A(Ca)$ because the available lines are widely spaced in wavelength over a region in which the instrument response changes by a factor of ~ 5.

III. DISCUSSION

We have catalogued over 60 spectral lines in the wavelength range 15.4-23.0 Å, a region not usually thought of as rich in line emission. The detection of Cr emission lines has been firmly established

31

for the first time. The strongest lines of Cr XV-XVI and Ca XV-XVIII are included in Table 1. The Cr and Ca spectra were found to be similar to the spectra of isoelectronic species of Fe. The newly catalogued lines will be useful in future emission measure analysis of solar coronal plasmas, especially for the range $T < 5 \times 10^6$ K.

To make optimum use of spectral lines for plasma diagnostics it is necessary to know the coronal element abundances. No single element provides lines for the entire temperature range ($\sim 2-30 \times 10^6$ K) found in coronal flare plasmas. X-ray spectrometry is a useful technique for abundance determination because the emitting structures are almost always optically thin and equation (1) is frequently applicable. Further, a worldwide effort in calculating the atomic physics parameters has been spurred by interest in fusion as an energy source. Table 2 shows the relative coronal abundances of the elements as determined from X-ray measurements ($A(O)=1$). The last two columns give relative abundances from Withbroe (1976) and Ross and Aller (1976).

The abundances of N, Ne, and Si are considered the most reliable. Each is based on a line ratio for which both lines have very similar emissivities as a function of T. All involve H- and He-like lines for which the emissivities are well understood. $A(Mg)/A(O)$ was obtained by multiplying $A(Mg)/A(Ne)$ (Rugge and Walker 1976) by $A(Ne)/A(O)$ (Acton, Catura, and Joki 1975). The Ca abundance is uncertain because of uncertainties in the emission measure $\epsilon(T)$. We also note that the expected density effects in the Ca XVI emission were not observed; the denser flare had relatively more Ca emission,

TABLE 2

Coronal Element Abundances Relative to Oxygen

Element	Abundance X-ray	Abundance Withbroe	Abundance Ross and Aller	X-ray Reference
N	0.14 ± 0.01	0.28	0.125	McKenzie et al. (1978)
Ne	0.21 ± 0.07	0.093	0.054	Acton, Catura, and Joki (1975)
Mg	0.15 ± 0.06	0.105	0.058	Rugge and Walker (1976)
Ca	0.015 ± 0.005	0.0081	0.0032	This work
Cr	0.0036 ± 0.0018	0.0087	0.0007	This work
Fe	----------	0.12	0.0457	

33

not less. If the emission was suppressed by density effects then A(Ca)/A(O) is understated in Table 2. The Cr abundance is uncertain because of approximations in the Cr ionization equilibrium and collision strength. We believe that 50% is a generous estimate of the combined errors. For Fe the uncertainty is large, for reasons given in §I.

From Table 2 it is clear that there is a great deal of disagreement among the various determinations of solar abundances. Although Ross and Aller (1976) consider A(O) among the best determinations, Withbroe's (1976) coronal abundance is a factor of 1.6 below his photospheric value and the Ross and Aller value. X-ray observations suggest that even Withbroe's coronal value may be high. Acton (1978) suggests that this value should be multiplied by 0.65. This recommendation is based on the O/Ne results cited above and on the work of Parkinson (1977) who derived the O/Si abundance ratio from X-ray observations. We note that if the Withbroe O abundance is multiplied by 0.65, his ratio A(Ca)/A(O) becomes 0.0125, which is in good agreement with ours. Our Cr abundance cannot be brought into agreement with either of the two compilations cited. The Ross and Aller value is certainly too low to account for our observed Cr line fluxes, and the Withbroe value is too high, especially if his A(O) is reduced by the recommended factor of 0.65. With the exception of the N/O ratio, none of the X-ray abundances relative to oxygen can be reconciled with the Ross and Aller values. Their Fe/Cr abundance ratio of 62 ± 26 is marginally in agreement with our value of 37 ± 18. The Cr lines might be used in conjunction with those of Fe to cover the temperature range

present in flares, especially if the Cr ionization equilibrium and collision strengths are calculated so that uncertainties in A(Fe)/A(Cr) are reduced. Similarly, for nonflaring tive regions, the lines of Cr XV can be used in conjunction with O VII and O VIII. Improved determinations of A(Fe)/A(O) are needed so that the lines of Fe XVII and Fe XVIII can be used to complete the analysis.

The spectra include density-sensitive Ca XV and Ca XVI lines. The latter will probably not be useful because no non-density-sensitive Ca XVI line is observable for comparison. The Ca XV lines are weak in our data and will usually only be useful if a number of SOLEX flare spectra are summed. This degrades the time resolution. Future spectrometers might easily achieve an order of magnitude higher sensitivity at ~ 22.7 Å by replacing the SOLEX channel electron multiplier array (post filter quantum efficiency < 10%) with a gas-flow proportional counter having a window similar to the SOLEX filters. Then individual flare spectra could be analyzed using the Ca XV lines. The Ca XV lines might be preferable to those of Ne IX, which lie in a wavelength range of strong Fe XIX emission and may be blended during flares (McKenzie et al. 1980b), for measurements of n_e at ~ 4×10^6 K. Theoretical line strength calculations are needed to allow optimum use of Ca XV density diagnostics.

REFERENCES

Acton, L. W. 1978, Ap. J., 225, 1069.

Acton, L. W., Catura, R. C., and Joki, E. G. 1975, Ap. J. (Letters), 195, L93.

Bearden, J. A. 1967, Revs. Mod. Phys., 39, 78.

Bhatia, A. K., Feldman, U., and Doschek, G. A. 1980, J. Appl. Phys., 51, 1464.

Bhatia, A. K., and Mason, H. E. 1981 (to be published).

Bromage, G. E., Cowan, R. D., Fawcett, B. C., Gordon, H., Hobby, M. G., Peacock, N. J., and Ridgeley, A. 1977, Culham Laboratory Report CLM-R 170.

Bromage, G. E., and Fawcett, B. C. 1977, M. N. R. A. S., 178, 591.

Burek, A. 1976, Space Sci. Instr., 2, 53.

Burkhalter, P. G., Cohen, L., Cowan, R. D., and Feldman, U. 1979, J. Opt. Soc. Am., 69, 1133.

Clark, R. E. H., and Magee, N. H. 1981, preprint.

Cohen, L., Feldman, U., and Kastner, S. O. 1968, J. Opt. Soc. Am., 58, 331.

Cowan, R. D. 1973, unpublished.

Craig, I. J. D., and Brown, J. C. 1976, Astr. Ap., 49, 239.

Doschek, G. A., Feldman, U., Kreplin, R. W., and Cohen, L. 1980, Ap. J., 239, 725.

Doschek, G. A., Feldman, U., Landecker, P. B., and McKenzie, D. L. 1981, Ap. J. (in press).

Eng, W., Jr., and Landecker, P. B. 1981, <u>Nucl. Instr. and Meth.</u> (in press).

Ermolaev, A. M., and Jones, M. 1973, British National Reference Library, Ref. No. SUP 70009.

Fawcett, B. C., and Hayes, R. W. 1975, <u>M.N.R.A.S.</u>, 170, 185.

Feldman, U., Doschek, G. A., Cowan, R. D., and Cohen, L. 1973, <u>J. Opt. Soc. Am.</u>, 63, 1445.

Gabriel, A. H., and Jordan, C. 1969, <u>M.N.R.A.S.</u>, 145, 241.

Garcia, J. D., and Mack, J. E. 1965, <u>J. Opt. Soc. Am.</u>, 55, 654.

Hutcheon, R. J., Pye, J. P., and Evans, K. D. 1976, <u>M.N.R.A.S.</u>, 175, 489.

Jacobs, V. L., Davis, J., Kepple, P. C., and Blaha, M. 1977, <u>Ap. J.</u>, 211, 605.

Jacobs, V. L., Davis, J., Rogerson, J. E., Blaha, M., Cain, J., and Davis, M. 1980, <u>Ap. J.</u>, 239, 1119.

Kelly, R. L. and Palumbo, L. J. 1973, <u>Atomic and Ionic Emission Lines Below 2000 Angstroms Hydrogen through Krypton</u> (Washington: Government Printing Office).

Landecker, P. B., McKenzie, D. L., and Rugge, H. R. 1979, <u>SPIE Proc.</u>, 184, 285.

Landini, M., and Fossi, B. C. Monsignori 1972, <u>Astr. Ap. Suppl.</u>, 7, 291.

Loulergue, M., and Nussbaumer, H. 1975, <u>Astr. Ap.</u>, 45, 125.

Magee, N. H., Jr., Mann, J. B., Merts, A. L., and Robb, W. D. 1977, Los Alamos Scientific Laboratory LA-6691-MS.

Mason, H. E. 1975, <u>M.N.R.A.S.</u>, 170, 651.

Mason, H. E., and Storey, P. J. 1980, M.N.R.A.S., 191, 631.

Mason, H. E., Doschek, G. A., Feldman, U., and Bhatia, A. K. 1979, Astr. Ap., 73, 74.

McKenzie, D. L., Broussard, R. M., Landecker, P. B., Rugge, H. R., Young, R. M., Doschek, G. A., and Feldman, U. 1980a, Ap. J. (Letters), 238, L43.

McKenzie, D. L., and Landecker, P. B. 1981, Ap. J. (in press).

McKenzie, D. L., Landecker, P. B., Broussard, R. M., Rugge, H. R., Young, R. M., Feldman, U., and Doschek, G. A. 1980b, Ap. J., 241, 409.

McKenzie, D. L., Rugge, H. R., Underwood, J. H., and Young, R. M. 1978, Ap. J., 221, 342.

Merts, A. L., Mann, J. B., Robb, W. D., and Magee, N. H., Jr. 1980, Los Alamos Scientific Laboratory LA-8267-MS.

Parkinson, J. H. 1977, Astr. Ap., 57, 185.

Pradhan, A. K., and Shull, J. M. 1981, preprint.

Ross, J. E., and Aller, L. H. 1976, Science, 191, 1223.

Rugge, H. R., and Walker, A.B.C., Jr. 1976, Ap. J. (Letters), 203, L139.

Sugar, J., and Corliss, C. 1977, J. Phys. Chem. Ref. Data, 6, 317.

———————————— 1979, J. Phys. Chem. Ref. Data, 8, 865.

Withbroe, G. L. 1976, Center for Astrophysics preprint, 524.

LABORATORY OPERATIONS

The Laboratory Operations of The Aerospace Corporation is conducting exper-
imental and theoretical investigations necessary for the evaluation and applica-
tion of scientific advances to new military space systems. Versatility and
flexibility have been developed to a high degree by the laboratory personnel in
dealing with the many problems encountered in the nation's rapidly developing
space systems. Expertise in the latest scientific developments is vital to the
accomplishment of tasks related to these problems. The laboratories that con-
tribute to this research are:

Aerophysics Laboratory: Launch vehicle and reentry aerodynamics and heat
transfer, propulsion chemistry and fluid mechanics, structural mechanics, flight
dynamics; high-temperature thermomechanics, gas kinetics and radiation; research
in environmental chemistry and contamination; cw and pulsed chemical laser
development including chemical kinetics, spectroscopy, optical resonators and
beam pointing, atmospheric propagation, laser effects and countermeasures.

Chemistry and Physics Laboratory: Atmospheric chemical reactions, atmo-
spheric optics, light scattering, state-specific chemical reactions and radia-
tion transport in rocket plumes, applied laser spectroscopy, laser chemistry,
battery electrochemistry, space vacuum and radiation effects on materials, lu-
brication and surface phenomena, thermionic emission, photosensitive materials
and detectors, atomic frequency standards, and bioenvironmental research and
monitoring.

Electronics Research Laboratory: Microelectronics, GaAs low-noise and
power devices, semiconductor lasers, electromagnetic and optical propagation
phenomena, quantum electronics, laser communications, lidar, and electro-optics;
communication sciences, applied electronics, semiconductor crystal and device
physics, radiometric imaging; millimeter-wave and microwave technology.

Information Sciences Research Office: Program verification, program trans-
lation, performance-sensitive system design, distributed architectures for
spaceborne computers, fault-tolerant computer systems, artificial intelligence,
and microelectronics applications.

Materials Sciences Laboratory: Development of new materials: metal matrix
composites, polymers, and new forms of carbon; component failure analysis and
reliability; fracture mechanics and stress corrosion; evaluation of materials in
space environment; materials performance in space transportation systems; anal-
ysis of systems vulnerability and survivability in enemy-induced environments.

Space Sciences Laboratory: Atmospheric and ionospheric physics, radiation
from the atmosphere, density and composition of the upper atmosphere, aurorae
and airglow; magnetospheric physics, cosmic rays, generation and propagation of
plasma waves in the magnetosphere; solar physics, infrared astronomy; the
effects of nuclear explosions, magnetic storms, and solar activity on the
earth's atmosphere, ionosphere, and magnetosphere; the effects of optical,
electromagnetic, and particulate radiations in space on space systems.